

# The 1.3 Å Crystal Structure of *Rhodobacter sphaeroides* Dimethyl Sulfoxide Reductase Reveals Two Distinct Molybdenum Coordination Environments

Hung-Kei Li, Carrie Temple,<sup>†</sup> K. V. Rajagopalan,<sup>†</sup> and Hermann Schindelin\*

Contribution from the Department of Biochemistry and Cell Biology, State University of New York at Stony Brook, Stony Brook, New York 11794-5215, and Department of Biochemistry, Duke University Medical Center, Durham, North Carolina 27710

Received February 22, 2000. Revised Manuscript Received May 19, 2000

**Abstract:** During the past four years, a substantial amount of structural information has been accumulated on the molybdoenzyme dimethyl sulfoxide (DMSO) reductase from purple bacteria. This enzyme contains a mono-nuclear Mo coordinated by two molybdopterin guanine dinucleotides as its single cofactor. Crystallographic studies on the enzyme from *Rhodobacter sphaeroides* and *Rhodobacter capsulatus* revealed substantial differences in the Mo coordination environment in the oxidized Mo(VI) state, despite a close structural similarity in the overall fold of the protein. The crystal structure of DMSO reductase from *R. sphaeroides* identified a Mo environment with a mono-oxo ligation and an asymmetric coordination by the two molybdopterin, with three short and one very long Mo–S bond. In contrast, two independent crystallographic studies of the enzyme from *R. capsulatus* revealed two additional Mo coordination environments: a pentacoordinated dioxo metal ligation sphere in which one molybdopterin is completely dissociated from the Mo and a heptacoordinated environment with symmetrical metal coordination by both molybdopterin and two oxo ligands. In all three structures the side chain of a serine was a ligand to the Mo. Adding to the controversy, EXAFS studies on the *R. sphaeroides* enzyme suggested a hexacoordinated active site geometry, whereas the same technique indicated seven ligands for the *R. capsulatus* enzyme. The 1.3 Å resolution crystal structure of oxidized DMSOR from *R. sphaeroides* presented here reveals plasticity at the active site. The Mo is discretely disordered and exists in a hexacoordinated and a pentacoordinated ligation sphere. The hexacoordinated model reconciles the existing differences in active site coordination of *R. sphaeroides* DMSO reductase as studied by crystallographic and EXAFS techniques. In addition, the pentacoordinated structure closely resembles one of the reported *R. capsulatus* crystal structures. In retrospect, the active site geometry in the previously reported 2.2 Å crystal structure of *R. sphaeroides* DMSO reductase appears to represent an average of the two conformations described here. Thus, structural flexibility at the active site appears to give rise to the observed differences in the Mo coordination environment.

## Introduction

The molybdenum cofactor (Moco)<sup>1,2</sup> is utilized in all phylogenetic kingdoms of life, and enzymes containing this cofactor are involved in a variety of important transformations in the global carbon, nitrogen, and sulfur metabolism.<sup>3,4</sup> Enzymes containing a Mo/W-pyranopterin cofactor are currently classified into four distinct families<sup>4</sup> and the structure of at least one member of each of these families has been characterized by X-ray crystallography.<sup>5–8</sup> The currently available crystal struc-

tures indicate that the Moco consists of one or two molecules of a tricyclic pyranopterin usually referred to as molybdopterin in which the metal is ligated to the sulfur atoms of one or two dithiolene groups. One of these four families is the DMSO reductase family and members of this family so far have been identified exclusively from eubacteria, and include dimethyl sulfoxide reductase, trimethylamine *N*-oxide reductase, biotin sulfoxide reductase, dissimilatory nitrate reductase, and formate dehydrogenase. DMSO reductase from either *Rhodobacter sphaeroides* or *Rhodobacter capsulatus* is an unusual molybdoenzyme in that it contains no cofactor other than Moco and consequently the enzyme has been studied by spectroscopic techniques which rely on the absorption properties of the cofactor.<sup>9–12</sup>

The crystal structure of oxidized Mo(VI) DMSO reductase from *R. sphaeroides* has been determined at 2.2 Å resolution.<sup>7</sup> Subsequently, the orthologous enzyme from *R. capsulatus* was independently characterized in its oxidized form by crystal-

\* To whom correspondence should be addressed at State University of New York at Stony Brook.

<sup>†</sup> Duke University Medical Center.

(1) Rajagopalan, K. V. *Adv. Enzymol.* **1991**, *64*, 215–290.

(2) Rajagopalan, K. V.; Johnson, J. L. *J. Biol. Chem.* **1992**, *267*, 10199–10202.

(3) Hille, R. *Chem. Rev.* **1996**, *96*, 2757–2816.

(4) Kisker, C.; Schindelin, H.; Rees, D. C. *Molybdenum—Cofactor Containing Enzymes: Structure and Mechanism*; Richardson, C. C., Ed.; Annual Reviews Inc.: Palo Alto, 1997; Vol. 66, pp 233–267.

(5) Chan, M. K.; Mukund, S.; Kletzin, A.; Adams, M. W. W.; Rees, D. C. *Science* **1995**, *267*, 1463–1469.

(6) Romão, M. J.; Archer, M.; Moura, I.; LeGall, J.; Engh, R.; Schneider, M.; Hof, P.; Huber, R. *Science* **1995**, *270*, 1170–1176.

(7) Schindelin, H.; Kisker, C.; Hilton, J.; Rajagopalan, K. V.; Rees, D. C. *Science* **1996**, *272*, 1615–1621.

(8) Kisker, C.; Schindelin, H.; Pacheco, A.; Wehbi, W. A.; Garrett, R. M.; Rajagopalan, K. V.; Enemark, J. H.; Rees, D. C. *Cell* **1997**, *91*, 973–983.

(9) Bastian, N. R.; Kay, C. J.; Barber, M. J.; Rajagopalan, K. V. *J. Biol. Chem.* **1991**, *266*, 45–51.

(10) Benson, N.; Farrar, J. A.; McEwan, A. G.; Thomson, A. J. *FEBS Lett.* **1992**, *2*, 169–172.

(11) Finnegan, M. G.; Hilton, J.; Rajagopalan, K. V.; Johnson, M. K. *Inorg. Chem.* **1993**, *32*, 2616–2617.

(12) Garton, S. D.; Hilton, J.; Oku, H.; Crousse, B. R.; Rajagopalan, K. V.; Johnson, M. K. *J. Am. Chem. Soc.* **1997**, *119*, 12906–12916.

lographic techniques at 1.88 Å<sup>13</sup> and 1.82 Å resolution.<sup>14</sup> Despite a close overall structural similarity among the proteins in the three crystal structures, there are surprisingly large differences in the coordination of the Mo. The structure of the *R. sphaeroides* enzyme<sup>7</sup> indicated a Mo environment with three short and one long Mo–S bond, a single oxo group, and the side chain oxygen of Ser 147. The coordination by the two dithiolene groups was found to be asymmetric. One pterin (P-pterin) coordinates the metal with both sulfurs at 2.4 Å distance. The sulfurs of the second pterin (Q-pterin) are 2.4 and 3.1 Å from the Mo. The first structure of the *R. capsulatus* enzyme<sup>13</sup> contained a pentacoordinated Mo ligated by the two sulfurs of only the P-pterin, two oxo groups, and the side chain of Ser 147. The second structure<sup>14</sup> contains a heptacoordinated metal bonded to the four dithiolene sulfurs in a symmetrical fashion, two oxo groups, and Ser 147. A comparison of the three crystallographic models indicated that it is mostly the position of the metal, which varies among the three models. In the *R. sphaeroides* enzyme the Mo is in an intermediate position, whereas it is maximally displaced (1.3 Å) between the two *R. capsulatus* structures. In addition, EXAFS studies of both enzymes have described six Mo ligands (four sulfurs, one oxo group, and one oxygen/nitrogen) for the *R. sphaeroides* enzyme,<sup>15,16</sup> but seven ligands (four sulfurs, two oxo, and one oxygen/nitrogen) for the *R. capsulatus* enzyme.<sup>17</sup> The interpretation of the *R. capsulatus* EXAFS data is however controversial.<sup>16</sup> Taken together, these studies describe coordination numbers ranging from 5 to 7 ligands, mono-oxo as well as di-oxo coordination environments, and both symmetric and asymmetric ligation by the four dithiolene sulfur atoms.

DMSO reductase catalyzes the conversion of DMSO to dimethyl sulfide (DMS). In addition, S- and N-oxides such as methionine sulfoxide, biotin sulfoxide, and trimethylamine-N-oxide are also substrates of the enzyme. Activities of *R. sphaeroides* DMSO reductase for DMSO, TMAO, methionine sulfoxide, clorate, biotin sulfoxide, and adenine-N-oxide are 3.6, 18.0, 4.3, 5.5, 4.8, and 7.1 units/nmol of Mo, respectively.<sup>18</sup> In the catalytic mechanism, which consists of an oxidative and a reductive half-reaction, the Mo cycles among the +IV, +V, and +VI oxidation states. The oxidative half cycle of the reaction is initiated by substrate binding to the reduced enzyme. In the catalytic step, the substrate oxygen is transferred as an oxo ligand to the Mo with a concomitant two-electron oxidation of the metal. Direct oxygen atom transfer was demonstrated by treating *R. sphaeroides* DMSO reductase with <sup>18</sup>O-labeled DMSO under single turnover conditions and subsequent transfer of the labeled oxygen to 1,3,5-triaza-7-phosphatricyclo[3.3.1.1]-decane, a water-soluble tertiary phosphine.<sup>19</sup> Resonance Raman spectroscopy confirmed these findings and showed that the oxo group could be labeled either by reoxidation of the dithionite reduced Mo(IV) sample after exchange into H<sub>2</sub><sup>18</sup>O buffer or by reoxidation with DMS<sup>18</sup>O in H<sub>2</sub><sup>16</sup>O.<sup>12</sup> After oxo transfer, the product DMS is released. The reductive half-cycle of the

reaction consists of two one-electron reduction steps coupled to the transfer of two protons to generate H<sub>2</sub>O from the substrate-derived oxo group. On the basis of the available structural data, the metal coordination geometry has been suggested to cycle between either des-oxo and mono-oxo or mono-oxo and di-oxo states. Therefore, the question of whether the active site of the oxidized enzymes has a mono-oxo or di-oxo geometry is directly relevant for the catalytic mechanism of the enzyme.

The structural discrepancies described above and their ambiguous mechanistic implications have prompted us to reexamine the active site geometry of *R. sphaeroides* DMSO reductase through a high-resolution crystallographic analysis. Here, we describe the 1.3 Å resolution crystal structure of *R. sphaeroides* DMSO reductase, which has been refined to a crystallographic *R*-factor of 0.121 (*R*<sub>free</sub> = 0.145). The Mo is discretely disordered and is present in either a hexacoordinated mono-oxo form, which is the catalytically relevant species, or a pentacoordinated di-oxo environment.

## Experimental Methods

**Protein Purification and Crystallization.** DMSO reductase from *R. sphaeroides* was purified as described recently.<sup>9,20</sup> A search for new crystallization conditions of *R. sphaeroides* DMSO reductase was initiated, starting with the known conditions<sup>7</sup> and a systematic variation of different additives. A new crystal form was obtained from a solution containing the enzyme at a concentration of 10 mg/mL in 10 mM Tris pH 7.5 and with 1.65 M (NH<sub>4</sub>)<sub>2</sub>SO<sub>4</sub>, 0.1 M HEPES pH 7.0, and 10 mM CdCl<sub>2</sub> as precipitant. Crystals were grown by hanging drop vapor diffusion and typically grew within 2 weeks to a size of 0.35 × 0.35 × 0.3 mm<sup>3</sup>. The new crystals belong to the orthorhombic space group *P*2<sub>1</sub>2<sub>1</sub>2 with *a* = 102.2 Å, *b* = 141.7 Å, and *c* = 59.8 Å and contain one molecule in the asymmetric unit. The Matthews' coefficient is 2.54 Å<sup>3</sup>/Da, which corresponds to a solvent content of 52%. At beamline X26C of the National Synchrotron Light Source (NSLS) at Brookhaven National Laboratory these crystals diffract X-rays to better than 1.3 Å resolution.

**Data Collection and Structure Solution.** For data collection, crystals were transferred into an artificial mother liquor containing 35% glucose (w/v) by stepwise increase in 5% increments and flash frozen in liquid nitrogen. Diffraction data were collected at 95 K on beamline X26C at the NSLS. A high-resolution dataset was collected on an ADSC Quantum IV CCD detector at a wavelength of 1.1 Å. The crystal-to-detector distance was 90 mm and a total of 400 images were collected, each with 0.25° oscillation range and 60 s exposure time. The data were indexed, integrated, and scaled with the HKL suite of programs.<sup>21</sup> Due to the detector geometry the diffraction data are less complete in the highest resolution shells (Table 1). The atomic coordinates of DMSOR from *R. sphaeroides* (PDB 1CX5) without the solvent molecules and the disordered residue Trp 388 were used to solve the new crystal form by molecular replacement with the program AMORE.<sup>22</sup> The rotation and translation functions were calculated with all data between 15.0 and 4.5 Å resolution and resulted in a unique solution with an *R*-factor of 0.361 and a correlation coefficient of 0.662. Subsequent rigid body refinement improved the *R*-factor and correlation coefficient to 0.344 and 0.719, respectively. The refined values for the rotational and translational parameters were  $\alpha = 20.87^\circ$ ,  $\beta = 61.14^\circ$ ,  $\gamma = 68.50^\circ$ ,  $t_x = 0.1486$ ,  $t_y = 0.2842$ , and  $t_z = 0.4453$ .

**Refinement.** Refinement of the model was carried out using the CCP4 suite of programs.<sup>23</sup> Initial refinement to 1.3 Å resolution of the model without solvent using REFMAC<sup>24</sup> resulted in an *R*-factor of 0.246

(13) Schneider, F.; Löwe, J.; Huber, R.; Schindelin, H.; Kisker, C.; Knäblein, J. *J. Mol. Biol.* **1996**, *263*, 53–69.

(14) McAlpine, A. S.; McEwan, A. G.; Shaw, A. L.; Bailey, S. *JBIC* **1997**, *2*, 690–701.

(15) George, G. N.; Hilton, J.; Rajagopalan, K. V. *J. Am. Chem. Soc.* **1996**, *118*, 1113–1117.

(16) George, G. N.; Hilton, J.; Temple, C.; Prince, R. C.; Rajagopalan, K. V. *J. Am. Chem. Soc.* **1999**, *121*, 1256–1266.

(17) Baugh, P. E.; Garner, C. D.; Charnock, J. M.; Collison, D.; Davies, E. S.; McAlpine, A. S.; Bailey, S.; Lane, I.; Hanson, G. R.; McEwan, A. G. *JBIC* **1997**, *2*, 634–643.

(18) Hilton, J. C.; Temple, C. A.; Rajagopalan, K. V. *J. Biol. Chem.* **1999**, *274*, 8428–8436.

(19) Schultz, B. E.; Hille, R.; Holm, R. H. *J. Am. Chem. Soc.* **1995**, *117*, 827–828.

(20) Hilton, J. C.; Rajagopalan, K. V. *Arch. Biochem. Biophys.* **1996**, *325*, 139–143.

(21) Otwinowski, Z.; Minor, W. *Processing of X-ray diffraction data collected in oscillation mode*; Carter, C. W., Sweet, R. M., Eds.; Academic Press: San Diego, 1997; Vol. 276, pp 307–326.

(22) Navaza, J. *Acta Crystallogr.* **1994**, *A50*, 157–163.

(23) Bailey, S. *Acta Crystallogr.* **1994**, *D50*, 760–763.

(24) Murshudov, G.; Vagin, A.; Dodson, E. *Acta Crystallogr.* **1997**, *D53*, 240–255.

**Table 1.** Data Collection and Refinement Statistics<sup>a</sup>

Data Collection Statistics	
resolution range (Å)	50.0–1.30 (1.35–1.30)
$R_{\text{sym}}$	0.051 (0.211)
completeness (%)	89.8 (60.2)
redundancy	3.6
$\langle I/\text{sig}I \rangle$	19.9 (2.2)
Refinement Statistics	
resolution range (Å)	10.0–1.30 (1.36–1.30)
$R$ -factor (%)	12.1 (16.1)
free $R$ -factor (%)	14.5 (18.7)
no. of reflns	186301
no. of atoms (protein/cofactor/solvent)	6050/163/1096
data-to-parameter ratio	2.83
dev from stereochemical ideality in	
bond lengths (Å)	0.010
bond angle distances (Å)	0.030
planar 1,4 distances (Å)	0.040
chiral volumes (Å <sup>3</sup> )	0.113
torsion angles (planar, staggered, orthonormal) (deg)	3.8/13.6/31.2
$B$ -factors (mc bond, mc angle, sc bond, sc angle) (Å <sup>2</sup> )	1.203/1.712/1.697/2.434
Ramachandran statistics (%)	89.1/10.3/0.5/0.2 (Glu 163)

<sup>a</sup> Numbers in parentheses are for the highest resolution shell, mc is main chain and sc is side chain. Ramachandran statistics were analyzed with the program PROCHECK<sup>35</sup> and percentages correspond to the most favored, additional allowed, generously allowed, and disallowed regions of the Ramachandran diagram.

( $R_{\text{free}} = 0.263$ ). At this point, disorder at the active site became evident. Subsequently, the active site was modeled in two alternate conformations including parts of both MGD's, the Mo, the side chains of Ser 147 and Tyr 114, and the oxo ligand that exists in both Mo coordination environments. Additional disordered side chains, not in the vicinity of the active site, were added subsequently. Model building using the program O<sup>25</sup> was carried out between refinement cycles. Automated addition of solvent molecules with the program ARP<sup>26</sup> and subsequent refinement using the program REFMAC yielded an  $R$ -factor of 0.171 ( $R_{\text{free}} = 0.192$ ). The final phase of refinement using the program REFMAC incorporated refinement of individual anisotropic  $B$ -factors. To validate the legitimacy of refining individual anisotropic  $B$ -factors, four different refinement protocols were carried out using the program SHELX.<sup>27</sup> The refinement protocols differed in the number of atoms for which anisotropic temperature factors were refined.

## Results

The overall structure of the enzyme has been described in detail elsewhere<sup>7</sup> and will be summarized only briefly. The enzyme is a mixed  $\alpha + \beta$  protein and the polypeptide fold consists of four domains grouped around the cofactor, which consists of two molybdopterin guanine dinucleotides (MGD). The four domains form a slightly elongated molecule with overall main chain dimensions of  $75 \times 55 \times 65 \text{ \AA}^3$ . The spatial arrangement of domains I to III creates a funnel-shaped depression on one side of the molecule. The active site is located at the bottom of the funnel. DMSO reductase contains two MGD molecules, named P- and Q-pterin, which coordinate the Mo with an approximate 2-fold axis of symmetry passing through the Mo. As first observed in the tungsten-containing aldehyde ferredoxin reductase from *Pyrococcus furiosus*,<sup>5</sup> each molybdopterin is present as a tricyclic pyranopterin. We use the atom numbering scheme for the tricyclic pyranopterin described in the initial structure.<sup>7</sup>

(25) Jones, T. A.; Zou, J. Y.; Cowan, S. W.; Kjeldgaard, M. *Acta Crystallogr.* **1991**, *A47*, 110–119.

(26) Perrakis, A.; Morris, R.; Lamzin, V. S. *Nat. Struct. Biol.* **1999**, *6*, 458–463.

(27) Sheldrick, G. M.; Schneider, T. R. *SHELXL: High-resolution refinement*; Carter, C. W., Sweet, R. M., Eds.; Academic Press: San Diego, 1997; Vol. 277, pp 319–343.

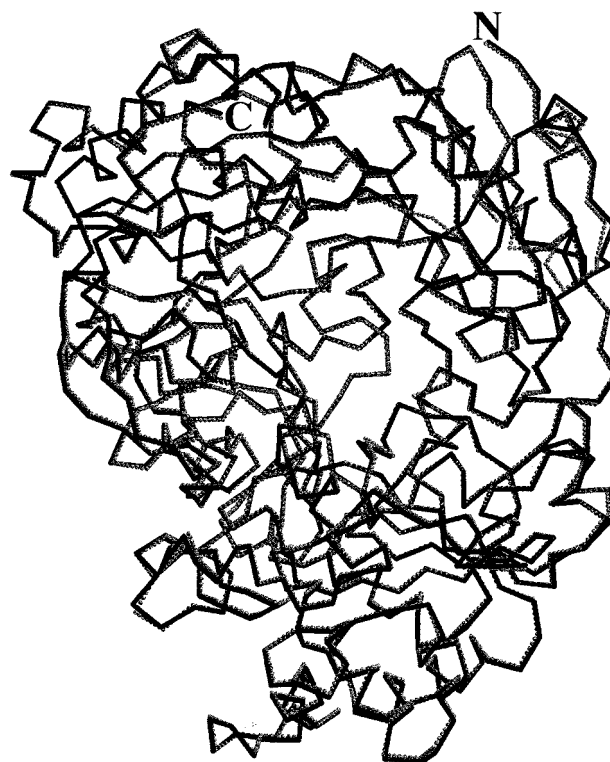


**Figure 1.** Superposition of the 1.3 (solid black) and 2.2 Å (dotted gray) resolution crystal structures of *R. sphaeroides* DMSO reductase. All figures were prepared with MOLSCRIPT<sup>33</sup> and RASTER3D.<sup>34</sup>

The structure of DMSO reductase has been refined at 1.3 Å resolution to an  $R$ -factor of 0.121 ( $R_{\text{free}} = 0.145$ ) including refinement of individual anisotropic temperature factors for all atoms in the model. The current model is comprised of residues 4 to 380, 384 to 385, and 393 to 780, two MGD's, 1 Mo, 1039 water, 3 glucose, 1 sulfate, and 1 Hepes molecule. As in the earlier model, the polypeptide loop comprising residues 380 to 394 is very mobile. Three residues, which were present at the N-terminus in the earlier structure, did not show electron density in the new maps and were excluded from the model. A superposition with the earlier 2.2 Å structure of *R. sphaeroides* DMSO reductase yields a root-mean-square (rms) deviation of 0.37 Å for 764 C $\alpha$  atoms, indicating no major structural changes (Figure 1). In the high-resolution structure, 34 residues are modeled with alternate conformations including the active site residues Ser 147 and Tyr 114. The validity of refining individual anisotropic temperature factors is demonstrated by alternative refinement protocols in which (a) no atoms, (b) only the heavy atoms (Cd, Mo, S, P), and (c) all atoms excluding the solvent molecules were refined anisotropically. The corresponding crystallographic and free  $R$ -factors are the following: (a)  $R = 0.157$  ( $R_{\text{free}} = 0.186$ ), (b)  $R = 0.156$  ( $R_{\text{free}} = 0.185$ ), and (c)  $R = 0.133$  ( $R_{\text{free}} = 0.172$ ). The lowest crystallographic and free  $R$ -factors ( $R = 0.121$  and  $R_{\text{free}} = 0.145$ ) were achieved with the refinement scheme including anisotropic temperature factor refinement of all atoms. Anisotropic refinement of all atoms leads to a data-to-parameter ratio of 2.83. If only isotropic temperature factors were to be refined, data to better than 1.8 Å resolution would be needed to obtain a similar data-to-parameter ratio. It should be pointed out that in the refinement of the *R. capsulatus* DMSO reductase structures which were refined at 1.82 and 1.88 Å resolution, refinement of isotropic temperature factors results in slightly lower data-to-parameter ratios of 2.56 and 2.26, respectively.

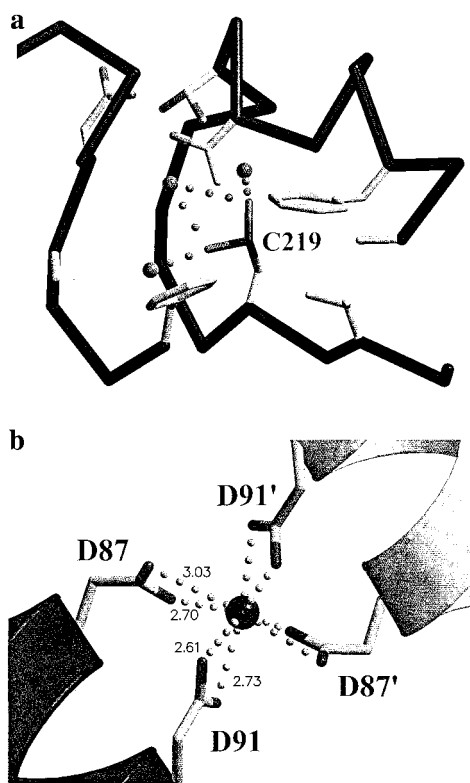


**Figure 2.** Novel structural features of DMSO reductase. (a) Environment of the sulfonic acid at position 219. (b) Cd-binding site at the monomer-monomer interface. One monomer is shown in black, the other in gray. Cadmium-ligand distances are given in Å.

The side chain of Cys 219 in *R. sphaeroides* DMSO reductase is covalently modified and is present as a sulfonic acid (Figure 2a). This residue is located in a rather hydrophobic environment and is surrounded by two phenylalanines, three alanines, two threonines, a valine, an aspartic acid, and three buried water molecules. The oxygens of the sulfonic acid are within hydrogen bonding distance to the three water molecules and to the amide nitrogen of Ala 228. The sulfur of the modified cysteine is 21.7 Å away from the Mo, precluding a functional role for this modified residue in the catalytic cycle of DMSO reductase. Furthermore, this residue is not conserved in *R. capsulatus* DMSO reductase where it is replaced by a valine. The presence of this modification could not be interpreted unambiguously in the earlier model, although some difference density around the sulfur of Cys 219 was observed.

**Cadmium-Binding Site.** In the new  $P2_12_12$  crystals, two DMSO reductase molecules dimerize along a crystallographic 2-fold axis of symmetry. This interaction is mediated by a Cd ion located on the 2-fold axis, which explains the requirement for  $\text{CdCl}_2$  in the crystallization solution. The cadmium interacts with the side chains of residues Asp 87 and Asp 91 from two adjacent DMSO reductase molecules (Figure 2b). The coordination geometry of the metal can be described as a distorted octahedron with Asp 87 O $\delta$ 1 (2.70 Å distance), Asp 91 O $\delta$ 1 (2.73 Å distance), and O $\delta$ 2 (2.61 Å distance) as ligands. In addition, O $\delta$ 2 of Asp 87 is 3.03 Å from the metal. Cadmium is commonly observed to have six ligands with octahedral coordination geometry, but can also occur with only five or four ligands. Due to the fact that the equatorial ligands originate from the same side chain (Asp 91), the bond angles in the equatorial plane deviate significantly from 90°. The interface between the two symmetry-related molecules is extremely small and only buries approximately 65 Å<sup>2</sup>. With the exception of the interac-

**Table 2.** Metal-Ligand Distances in the Hexa- and Pentacoordinated Forms of *R. Sphaeroides* DMSO Reductase

	hexacoordinated	pentacoordinated
geometry	distorted trigonal prismatic	square pyramidal
Mo-S1' P (Å)	2.45	2.50
Mo-S2' P (Å)	2.38	2.45
Mo-S1' Q (Å)	2.45	not a ligand
Mo-S2' Q (Å)	2.42	not a ligand
Mo-Ser 147 O $\gamma$ (Å)	1.84	1.92
Mo-Oxo1 (Å)	1.76	1.75
Mo-Oxo2 (Å)	not a ligand	1.71

tions via the cadmium there are no other direct contacts between the two molecules. This clearly indicates that the dimerization is due to packing interactions and is not of functional significance. The cadmium is separated by 38.7 Å from the Mo and is not in close proximity to the active site of DMSO reductase.

**Active Site Disorder.** The initial model used for refinement did not contain any oxo ligands, but did contain the metal and the two MGD's. Initial electron density maps revealed disorder at the active site, and two alternate positions of the Mo were immediately apparent. The metal refined to the position of the major conformer and a very large difference density peak was observed at a distance of 1.6 Å from the Mo. An atom placed at this position was within a distance of roughly 2.5 Å from all four dithiolene sulfurs of the two pterins. This fact and the height of the peak in the difference density suggested that this peak could represent an additional location of the Mo (Figure 3). After inclusion of the Mo at the second site, additional less electron-rich ligands were included in the model. One oxygen is a ligand in both coordination environments, but is displaced by 0.78 Å between its two positions. Initially, this atom was not refined with alternate conformations. However, additional difference density on either side of the average oxygen position indicated disorder. An additional oxygen atom, which is only present in one of the two conformations, was included in the vicinity of Tyr 114. To make room for this ligand, the side chain of Tyr 114 has to shift and consequently this residue, in addition to Ser 147, is also disordered. The Mo in the two metal coordination sites is either pentacoordinated or hexacoordinated. The detailed environments will be described below and are summarized in Table 2. The occupancies for the two alternate conformations were adjusted to 0.6 and 0.4 for the penta- and hexacoordinated Mo conformations, respectively, based on the thermal factors of corresponding atoms.

**Hexacoordinated Environment.** In this conformation the Mo is ligated by four ligands which originate from the sulfurs of the two dithiolene groups with an average ligand-to-metal distance of 2.43 Å (the individual values range from 2.38 to 2.45 Å). In addition, an oxo ligand at a distance of 1.76 Å and the side chain oxygen of Ser 147 at 1.84 Å complete the coordination sphere. The coordination of the Mo can be described as a distorted trigonal prism, where each trigonal face is formed by two sulfurs from opposite dithiolenes and one oxygen atom (Figure 4a). The sulfur-to-sulfur distances are 3.14 and 3.09 Å within the same dithiolene group and 3.55 and 3.32 Å between adjacent sulfur atoms from opposite dithiolene groups. The oxo ligand is not trans to any of the dithiolene sulfurs, and therefore no weakening of the Mo-S bonds as a consequence of the well-documented trans-effect is expected. The Mo environment described above is related to the active site in the heptacoordinated *R. capsulatus* structure<sup>14</sup> with the significant exception of the additional oxo ligand which is present only in the *R. capsulatus* model (Figure 4b). The Mo and the two coordinating MGD's can be superimposed with

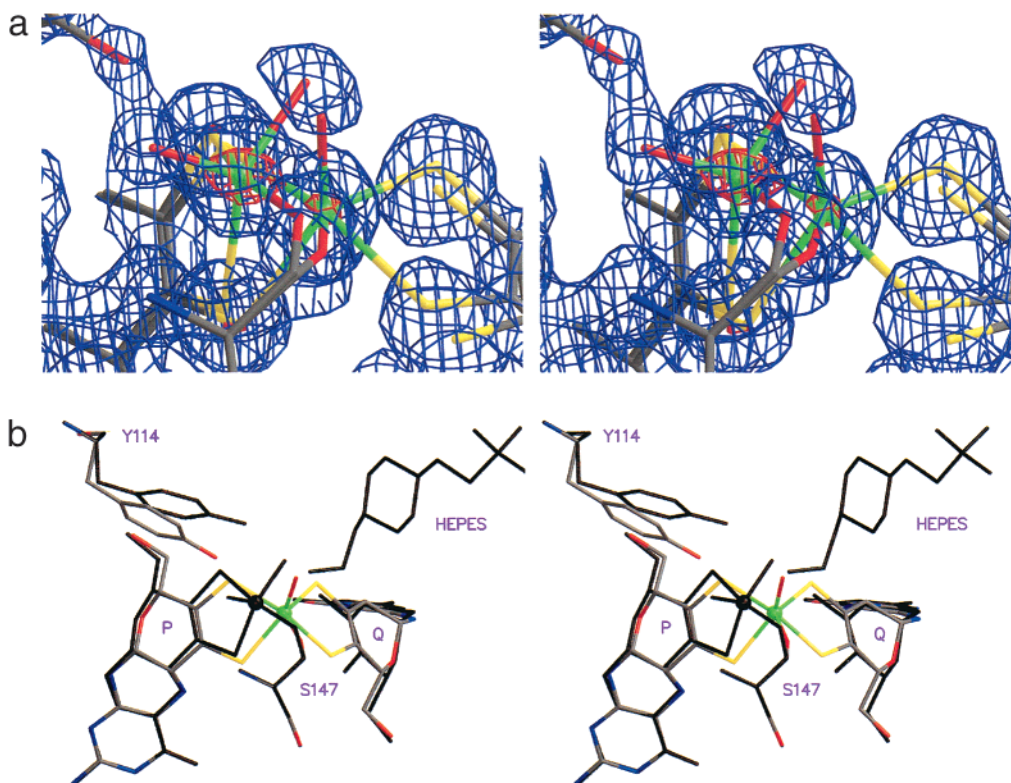


**Figure 3.** Active site structure of DMSO reductase. (a) Electron density maps around the Mo. A SIGMAA weighted  $2F_o - F_c$  electron density map is displayed at two contour levels (blue =  $1\sigma$ , red =  $16.6\sigma$ ) and is superimposed with the refined model. Different atom types are color coded with Mo in green, S in yellow, P in purple, O in red, N in blue, and C in gray. The density feature in the upper left corner indicates the hydroxyl group of Tyr 114 as present in the hexacoordinated structure. (b) Stereorepresentation of the two coordination environments including Tyr 114 and the bound HEPES molecule. The hexacoordinated Mo environment is shown in color, the pentacoordinated environment in black.

root-mean-square deviations of  $0.19\text{ \AA}$ . Interestingly, the position of the additional oxo ligand in the *R. capsulatus* structure is almost identical to the position of the Mo in the pentacoordinated model described below.

**Pentacoordinated Environment.** In the second conformation, the Mo is pentacoordinated: Only two sulfur ligands, both from the P-pterin, remain at distances of  $2.50\text{ \AA}$  ( $S1'$ ) and  $2.45\text{ \AA}$  ( $S2'$ ). The sulfurs of the Q-pterin are at distances of  $3.62\text{ \AA}$  ( $S1'$ ) and  $4.53\text{ \AA}$  ( $S2'$ ), respectively, too far away for direct interactions with the Mo. Two oxo groups at distances of  $1.75\text{ \AA}$  (oxo1) and  $1.71\text{ \AA}$  (oxo2) as well as the side chain of Ser 147, which remains ligated to the Mo ( $1.92\text{ \AA}$  distance), complete the coordination sphere. Oxo1 is the common oxo group also observed in the hexacoordinated form, whereas oxo2 is not present in the hexacoordinated form. The coordination geometry can be described as square pyramidal with the Mo at the center of the pyramid and the additional oxo ligand (oxo2) at the tip of the pyramid (Figure 5a). This ligand is trans to the dithiolene group of the Q-pterin and the observed increase in the Mo–S bond lengths is in agreement with the trans effect of this ligand. The atoms forming the base of the pyramid are separated from each other by  $3.20\text{ \AA}$  ( $S1'$  and  $S2'$ ),  $3.26\text{ \AA}$  ( $S1'$  and  $O\gamma$ ),  $2.58\text{ \AA}$  ( $O\gamma$  and oxo1), and  $2.87\text{ \AA}$  (oxo1 and  $S1'$ ). The Mo is displaced by  $0.66\text{ \AA}$  from a least-squares plane fitted through  $S1'$ ,  $S2'$ ,  $O\gamma$ , and oxo1. The oxo1–Mo–oxo2 bond angle is  $104.8^\circ$ , which is close to the average value of  $106^\circ$  observed in dioxomolybdenum containing model compounds.<sup>28</sup> The pentacoordinated Mo environment is very similar to the coordination environment described by Schneider et al.<sup>13</sup> for the *R. capsulatus* enzyme (Figure 5b). The Mo and the two coordinating MGD's can be

superimposed with a root-mean-square deviation of  $0.21\text{ \AA}$ . The major difference between the pentacoordinated *R. sphaeroides* and *R. capsulatus* structures is the separation of the two sulfurs in the Q-pterin, which is shortened by  $0.7\text{ \AA}$  in the *R. capsulatus* structure. At a sulfur-to-sulfur distance of  $2.5\text{ \AA}$ , a partial disulfide bond appears to have formed in the *R. capsulatus* structure. In addition, this pentacoordinated Mo environment is also rather similar to the inactive de-sulfo form of the aldehyde oxidoreductase from *Desulfovibrio gigas*.<sup>6</sup> An earlier  $1.35\text{ \AA}$  crystal structure of *R. sphaeroides* DMSO reductase, briefly described in Rees et al.,<sup>29</sup> revealed a Mo coordination that is nearly identical to the pentacoordinated structure described here. The crystals used in this study belonged to the original  $P2_12_12_1$  crystal form,<sup>7</sup> but were soaked in mother liquor containing 35% glycerol as cryo-protectant to allow data collection at cryogenic temperatures. Although the model could be refined to comparably low *R*-factors as the structure described here, additional density features around the metal and one of the dithiolene sulfurs make a satisfactory interpretation of this form problematic. As mentioned earlier,<sup>29</sup> one possible scenario is the oxidation of one of the dithiolene sulfurs to a sulfenic acid, but even this modification cannot fully explain the electron density at the active site and thus this assignment has to be viewed with caution.

## Discussion

The major difference between the two coordination environments observed in this structure is a displacement of the Mo by  $1.6\text{ \AA}$ . A similar movement is also apparent from a superposition of the two *R. capsulatus* structures, which reveals

(28) Stiefel, E. I. In *Comprehensive Coordination Chemistry*; Wilkinson, G., Ed.; Pergamon Press: Oxford, U.K., 1987; pp 1375–1420.

(29) Rees, D. C.; Hu, Y.; Kisker, C.; Schindelin, H. *J. Chem. Soc., Dalton Trans.* **1997**, 21, 3909–3914.

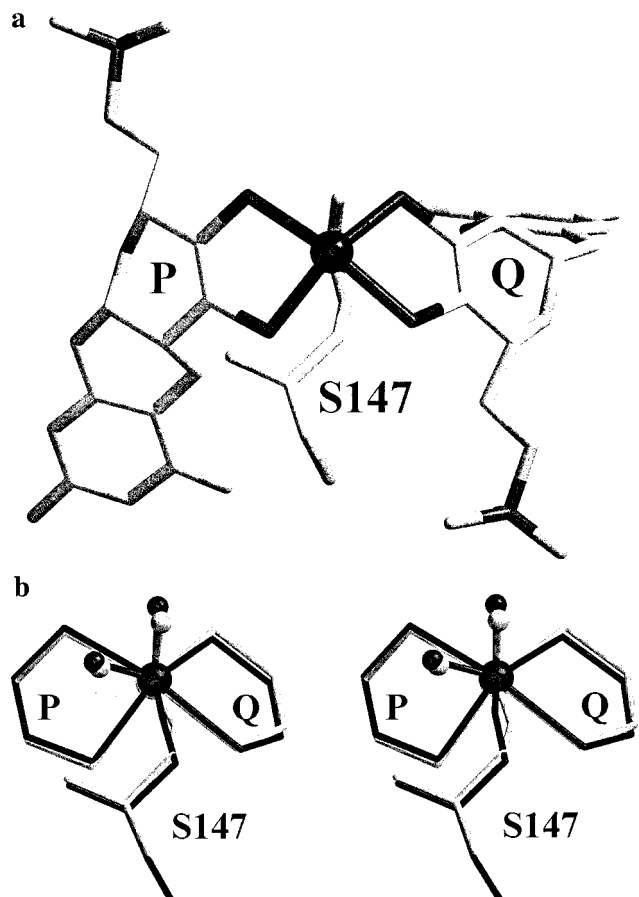


**Figure 4.** Hexacoordinated Mo environment. (a) Representation of the hexacoordinated Mo-environment. The P- and Q-pterins are shown without their attached guanosine monophosphate moieties. Different atom types are shown in different shades of gray. (b) Stereorepresentation of a superposition of the hexacoordinated Mo environment in *R. sphaeroides* DMSO reductase (light gray) with the hexacoordinated Mo environment in *R. capsulatus* DMSO reductase (black). Only the dithiolene groups, Ser 147, and the oxo-ligands are shown. The alternate position of the Mo in *R. sphaeroides* DMSO reductase is indicated as a gray sphere and this atom superimposes with the additional oxo-ligand in the *R. capsulatus* structure.

a 1.3 Å shift in the Mo position. In the high-resolution structure, additional structural rearrangements are observed in both pterins besides the displacement of the Mo. Whereas these changes affect the entire tricyclic Q-pterin, the pyrophosphate linkage, and the ribose of the guanosine, they do not extend beyond the pyrophosphate linkage in the P-pterin. The side chain of Ser 147 adjusts to the different positions of the Mo through a 26° rotation around the C $\alpha$ -C $\beta$  bond. In addition, the side chain of Tyr 114 adopts a different conformation to make room for the additional oxo ligand present only in the pentacoordinated structure. The structure also reveals a Hepes buffer molecule bound at the active site, which is pointing with its hydroxyethyl side chain toward the Mo. The pyrazine ring is stacked between the aromatic side chains of Tyr 145 and Trp 195 and the ethane-sulfonic acid moiety is pointing toward the solvent. On the basis of its temperature factors, the Hepes molecule appears to have partial occupancy and is present only in the pentacoordinated state. The distance between the carbon to which the terminal hydroxyl group is connected and the oxo ligand in the hexacoordinated structure would be only 2.96 Å, which is slightly smaller than the sum of the van der Waals radii. In the pentacoordinated structure, these two atoms are separated by

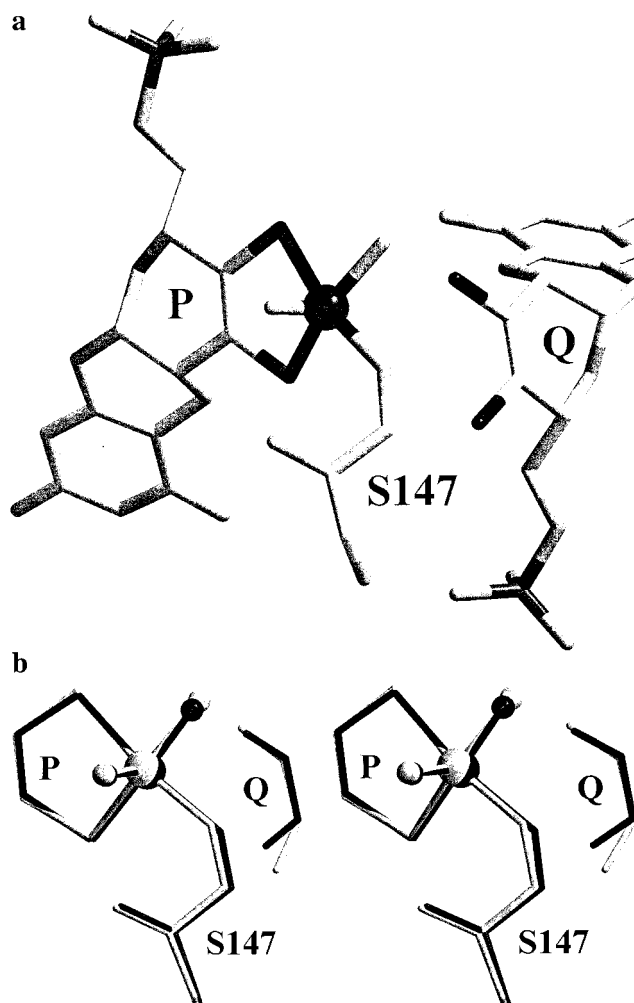


**Figure 5.** Pentacoordinated Mo environment. (a) Representation of the pentacoordinated Mo environment. The P- and Q-pterins are shown without their attached guanosine monophosphate moieties. Different atom types are shown in different shades of gray. (b) Stereorepresentation of a superposition of the pentacoordinated Mo environment in *R. sphaeroides* DMSO reductase (light gray) with the pentacoordinated Mo environment in *R. capsulatus* DMSO reductase (black). Only the dithiolene groups, Ser 147, and the oxo-ligands are shown.

3.15 Å. It seems as if the bound Hepes molecule induces the structural change in the Mo-coordination environment to eliminate this unfavorable interaction.

In hindsight, the 2.2 Å crystal structure of *R. sphaeroides* DMSO reductase can be interpreted as a superposition of the two independent conformations described above, which could not be resolved at the lower resolution of the earlier study. To test this hypothesis we truncated the diffraction data at 2.2 Å resolution and calculated electron density maps with the corresponding subset of reflections. The resulting maps did not resolve the individual positions of the Mo and instead indicated an average position, which closely corresponds to the position of the metal in the initial structure. Even truncating at a higher resolution, comparable to the *R. capsulatus* structures, does not resolve two independent positions of the Mo, but instead, reveals an extended density feature covering the individual locations of the metal. The superposition of our hexacoordinated model with the heptacoordinated *R. capsulatus* model positions the additional oxo ligand of the *R. capsulatus* model on top of the Mo position in the pentacoordinated structure. This observation raises the possibility that the additional oxo ligand in the heptacoordinated *R. capsulatus* structure in fact represents a

minor alternate conformation of the metal. The discrete disorder would have not been detected due to the lower resolution of this study, which could be further compounded if this conformation is only populated at a small percentage. This explanation would also eliminate the criticism put forward by George et al.<sup>16</sup> regarding the unusual interactions in which the additional oxygen in the heptacoordinated structure of *R. capsulatus* DMSO reductase is involved. Further support for this hypothesis is provided by a comparison of the Mo displacements of 1.6 and 1.3 Å in the *R. sphaeroides* and *R. capsulatus* structures, respectively. The 0.3 Å difference between these two values is mostly due to a shift of the Mo in the heptacoordinated *R. capsulatus* structure toward the additional oxo ligand when compared to the hexacoordinated model. If disorder were present in the structure described by McAlpine et al., the average position of the metal would be shifted in the direction observed.

A comparison of the new results with the published EXAFS data<sup>15,16</sup> resolves some of the existing controversy regarding the Mo coordination in *R. sphaeroides* DMSO reductase. The hexacoordinated Mo environment is in very good agreement with the published EXAFS data on the oxidized form of the enzyme. Even the metal–ligand distances are reproduced quite accurately. The average Mo–S distances are 2.425 Å in the crystal structure compared to 2.435 Å in the EXAFS model. The value for the oxo ligand is slightly larger (1.76 Å compared to 1.68 Å), whereas the distance to the oxygen of the Ser side chain is slightly smaller with 1.84 Å compared to the distance of 1.92 Å to the additional oxygen described in the EXAFS analysis. For comparison, crystallographic<sup>30</sup> and EXAFS<sup>31</sup> analyses of a mono-oxo-containing model compound mimicking the active site of DMSO reductase revealed a metal-to-oxo distance of 1.72 Å. It should be pointed out that the oxo1 ligand is the least accurately determined atom in the Mo-coordination sphere. This is due to the fact that the two alternate positions of this atom are within 0.78 Å and cannot be resolved. In addition, this atom is not covalently bound to any other atom and consequently there are no stereochemical restraints, which can be employed to restrain its position. Despite the fact that the crystal structure described here was determined at 1.3 Å resolution its accuracy is still not at the level of small molecule crystal structures and presumably the macromolecular EXAFS analysis. Estimates of the average coordinate error indicate an overall coordinate error of 0.04 Å based on Cruickshank's formula or 0.02 Å based on the maximum likelihood formalism as estimated by the refinement program. Slight discrepancies in bond lengths between the crystal structure of DMSO reductase and the EXAFS data are, therefore, within the experimental errors. In addition, series termination effects in the Fourier transformations lead to density artifacts around electron dense scatterers,<sup>32</sup> which could influence the exact position of Mo ligands and might lead to an overestimation of bond distances.

Resonance Raman spectroscopic characterization of *R. sphaeroides* DMSO reductase<sup>11</sup> has indicated that all four sulfurs are ligands to the Mo, but has suggested a difference in the electronic state of the two dithiolenes. One was described as a

dithiolate ligand, while the other has more  $\pi$ -delocalized character. Based on this assignment one would predict for the dithiolene group of one of the pterins a short carbon–carbon distance consistent with a double bond and, at the same time, a carbon–sulfur bond length consistent with a single bond. In contrast, the dithiolene group of the other pterin should have an increased carbon–carbon distance indicating a diminished double bond character and a decrease in the carbon–sulfur bond lengths. At the current resolution of our crystallographic model, we do observe small geometric differences in the two dithiolenes in the hexacoordinated form, which are consistent with this distinction. In the P-pterin, the C–S bonds are 1.73 (C1' to S1') and 1.78 Å (C2' to S2') with a C1'–C2' bond length of 1.36 Å. In the Q-pterin, the C–S bonds are slightly longer, 1.77 (C1' to S1') and 1.81 Å (C2' to S2'). At the same time the C1'–C2' bond is slightly shorter (1.34 Å). These observations would assign the P-pterin as the one having more  $\pi$ -delocalized character and the Q-pterin as having an ene-dithiolate electronic state in agreement with the assignment deduced by Resonance Raman spectroscopy.

As stated earlier, the presence of Hepes appears to have induced the change in Mo coordination leading to the pentacoordinated form described here, which is supported by the following observation. If Hepes is replaced by cacodylic acid, but no additional changes are made to either the mother liquor or the cryosolutions, the pentacoordinated state completely disappears (H.-K.L., C.T., K.V.R., and H.S., unpublished data). The pentacoordinated form has been independently observed in one of the *R. capsulatus* structures<sup>13</sup> and the 1.35 Å structure of *R. sphaeroides* DMSO reductase.<sup>29</sup> Furthermore, the original room temperature structure of *R. sphaeroides* DMSO reductase<sup>7</sup> most likely contained a mixture of a hexacoordinated and a pentacoordinated Mo. The question arises as to what could have caused the corresponding change in Mo coordination in these other structures. A comparison of the crystallization conditions reveals the presence of 2-methyl-2,4-pentanediol (MPD) in the precipitants for the *R. capsulatus* crystal form of Schneider et al.<sup>13</sup> and the original crystal form of *R. sphaeroides* DMSO reductase.<sup>7</sup> In the case of the *R. capsulatus* enzyme, the MPD concentration was 30%, whereas it was around 3% for the *R. sphaeroides* enzyme. Consistent with the concentrations of MPD, either a complete (*R. capsulatus* structure) or a partial conversion (*R. sphaeroides* structure) into the pentacoordinated form is observed. MPD therefore appears to induce the conversion from the catalytically active hexacoordinated Mo environment to the pentacoordinated environment. Furthermore, the 1.35 Å crystal structure was derived from crystals containing 3% MPD, but these crystals were subsequently soaked in mother liquor which was supplemented with 35% glycerol as cryoprotectant. Given the close structural similarity between glycerol and MPD, it is probably not surprising that the addition of glycerol induced a similar change as the one observed in the presence of MPD. Consequently, addition of either MPD, or glycerol, or Hepes appears to induce the transition from the active hexacoordinated Mo environment to the pentacoordinated form. At present, all substances that induce this transition are required at rather high concentrations and the observed structural change does not appear to be of physiological relevance.

The high-resolution crystal structure of *R. sphaeroides* DMSO reductase resolves the existing controversy regarding the metal coordination in this enzyme. The catalytically competent form of the oxidized enzyme features a mono-oxo active site with close to symmetrical coordination by four dithiolene sulfurs and a sixth ligand originating from the side chain of Ser 147. This

(30) Donahue, J. P.; Goldsmith, C. R.; Nadiminti, U.; Holm, R. H. *J. Am. Chem. Soc.* **1998**, *120*, 12869–12881.

(31) Musgrave, K. B.; Donahue, J. P.; Lorber, C.; Holm, R. H.; Hedman, B.; Hodgson, K. O. *J. Am. Chem. Soc.* **1999**, *121*, 10297–10307.

(32) Schindelin, H.; Kisker, C.; Rees, D. C. *JBIC* **1997**, *2*, 773–781.

(33) Kraulis, P. J. *J. Appl. Crystallogr.* **1991**, *24*, 946–950.

(34) Merritt, E. A.; Bacon, D. J. *Raster3D: Photorealistic Molecular Graphics*; Carter, C. W., Sweet, R. M., Eds.; Academic Press: San Diego, 1997; Vol. 277, pp 505–524.

(35) Laskowski, R. A.; McArthur, M. W.; Moss, D. S.; Thornton, J. M. *J. Appl. Crystallogr.* **1993**, *26*, 283–291.

structure is consistent with the catalytic mechanism suggested on the basis of the resonance Raman data<sup>12</sup> and the catalytically labile oxygen is the single oxo group located opposite the side chain of Ser 147. Not surprisingly, this oxygen is the most accessible of all atoms in the cofactor. The second conformation of the active site in which the Mo is coordinated only by two sulfurs of the P-pterin, two oxo-groups, and the side chain of Ser 147 reproduces one of the available *R. capsulatus* DMSO reductase structures. Furthermore, the presence of two independent conformations suggests that the *R. capsulatus* structure in which the metal is heptacoordinated might be a result of disorder that was not obvious at the lower resolution of this study.

**Acknowledgment.** Supported by National Institutes of Health Grants DK54835 (H.S.) and GM00091 (K.V.R.). H.S. thanks Dr. Douglas C. Rees for his generosity and the Department of Pharmacological Sciences at SUNY Stony Brook for its hospitality. The National Synchrotron Light Source in Brookhaven is supported by the United States Department of Energy and the National Institute of Health, and beamline X26C is supported in part by the State University of New York at Stony Brook and its Research Foundation. The atomic coordinates have been deposited in the Protein Data Bank (PDB 1EU1).

JA000643E